Decomposed LT Codes for Cooperative Relay Communications

Rui Cao, *Student Member, IEEE* and Liuqing Yang, *Senior Member, IEEE*

***Abstract*—Forward error correction (FEC) is commonly adopted in cooperative relay communications to ensure link-layer communication reliability. Among those schemes, rateless fountain codes, such as Luby Transform (LT) codes, are favorable for their low complexity and rate adaptability to channel fading dynamics. However, the cooperative transmission schemes based on primitive fountain codes induce either heavy computation cost or large end-to-end latency. To address these issues, we explore decomposed LT (DLT) codes, which comprise of two layers of random encoding but only a single layer of decoding. By implementing the two layers of encoding at the source and the relay(s) respectively, the cooperative system can ensure communication reliability on both source-relay and relay-destination links with reduced computation cost and latency. In this work, we first develop a general decomposition technique for the DLT code construction. Based on this, we further propose a hybrid decomposition algorithm tailored for LT codes with robust Soliton distribution (RSD). The resultant hybrid DLT (h-DLT) codes facilitate flexible computation cost allocation. The h-DLT codes based cooperative relay communication protocol is then developed and analyzed in terms of the transmission latency and energy consumption.**

***Index Terms*—Cooperative relay communications, LT codes, distribution decomposition, forward error correction.**

I. Introduction

TO COMBAT channel fading in wireless networks, cooperative relay communications have been extensively studied in the literature to enhance communication reliability and extend range [1]. In cooperative relay communications, several intermediate nodes are employed to collaboratively deliver the information from the source to the destination. By utilizing spatial diversity, various reliable communication protocols have been designed at the physical layer [1], [2].

From the networking perspective, the inherent dual-hop wireless transmission nature of cooperative relay communications induces some unique requirements on the protocol design. First, due to the independent channel fading on source-relay and relay-destination links, the transmission reliability needs to be assured for both hops [3]. Secondly, the end-to-end data delivery latency needs to be reduced, especially for delay-sensitive applications [4]. Thirdly, heterogeneous node energy is a critical factor that limits the network lifetime. In the literature, residual-energy-aware relay selection protocols are designed to cope with this problem [5], [6], while the hybrid automatic retransmission request (ARQ) scheme is commonly adopted to address the first two issues [7], [8]. By transmitting redundant coded packets using forward error correction (FEC) codes, hybrid ARQ schemes can ensure the communication reliability with significantly reduced retransmission. Various FEC codes have been developed. Examples includes Reed−Solomon (RS) codes and Tornado codes [9]. More recently, rateless fountain codes [10] are also proposed to reduce computation cost and enable code rate adaptability.

In [3], [11], [12], independent fountain encoding is adopted at each hop to ensure the dual-hop transmission reliability. Thus the relays need to decode and re-encode each received packet, and send acknowledgements (ACKs) back to the source to confirm each correct reception. Clearly, high computation cost is required at the relays and large transmission latency is induced by the frequent feedback messages. To address these issues, concatenated encoding is adopted in [13], [14], [15], [16], where the relay nodes simply apply a second-layer of coding to the fountain-coded source data without decoding. In [14], several relay encoding schemes are designed and compared. The fixed-rate systematic codes require the relay-destination channel erasure information feedback, which introduces additional latency; and the greedy random codes have low latency but impose high decoding complexity at the destination. In [13], an online fountain encoding scheme is developed for the relay at the cost of increased storage requirement. In [16], random linear fountain codes are used at both the source and relays. A spectral-efficient relaying protocol is also designed for a two-relay cooperative system. This work is extended to multi-relay systems in [15]. Clearly, all cooperative transmission protocols based on concatenated coding entail significant decoding complexity at the destination.

In order to reduce computation complexity and latency while retaining communication reliability on both links using fountain codes, the concept of decomposed fountain codes has been proposed. Typically, the decomposed fountain codes consist of two layers of data encoding which can be performed collaboratively by the source and intermediate relay nodes. In particular, analysis in [17] shows that the asymptotic performance of decomposed LT (DLT) codes with two-layer random encoding is the same as that of the corresponding non-decomposed LT code. The first DLT code is the so termed distributed LT [18], which is essentially a special DLT

Manuscript received 22 June 2011; revised 20 July 2011. Part of the results in this paper is presented at the IEEE Global Communications Conference (GLOBECOM), Houston, TX, 2011, and the IEEE Military Communications Conference (MILCOM), Baltimore, MD, 2011. This work is in part supported by National Science Foundation under grant #1129043 and Office of Naval Research under grant #N00014-11-1-0667.

R. Cao is with the Department of Electrical and Computer Engineering, University of Florida, Gainesville, FL 32611, USA, (e-mail: raycao@ufl.edu; phone: 352-392-9469; fax: 352-392-0044).

L. Yang is with the Department of Electrical and Computer Engineering, Colorado State University, Fort Collins, CO 80523, USA, (e-mail: lqyang@engr.colostate.edu; phone: 970-491-6215; fax: 970-491-2249).

Digital Object Identifier 10.1109/JSAC.2012.120220.

code with the second-layer encoding degree fixed to 2 or 4. However, the fixed-degree encoding at the second layer encoding limits the application of the distributed LT codes in cooperative relay communications, due to the compromised communication reliability on the second hop.

In this work, we will develop generalized DLT codes for cooperative relay communications. First, a general DLT code construction approach is investigated based on polynomial decomposition. Due to the spiky feature of the classical robust Soliton distribution (RSD) [19], a hybrid decomposition algorithm is then developed. The resultant hybrid DLT (h-DLT) codes enable flexible computation cost allocation between two encoders, thus they can readily cope with the node energy heterogeneity issue in cooperative networks. Based on the h-DLT codes, a reliable cooperative communication scheme (DLT-CC) is designed, by seamlessly incorporating the two-layer h-DLT encoding into the dual-hop communications. With our DLT-CC scheme, random encoding at both the source and the relays ensures communication reliability on both links. Secondly, the rate adaptation on both links enables reduced transmission latency and communication cost. Thirdly, low computation complexity can be achieved at all nodes due to the decomposed encoding and the single-layer decoding. Finally, by carefully choosing the h-DLT encoding ratio according to the relative residual energy of the cooperative nodes, the computation cost can be flexibly balanced.

The rest of the paper is organized as follows. The DLT code construction is investigated in Sec. II, and the h-DLT codes are developed for the RSD in Sec. III. Then the DLT-CC protocol and its performance will be presented in Sec. IV. Summarizing remarks will be given in Sec. V.

II. Decomposed LT (DLT) Codes

The DLT codes are derived from the primitive LT codes, but featured with two layers of encoding. In this section, we will briefly review the LT codes. Then the DLT code construction is investigated through polynomial decomposition.

A. LT codes

Fountain codes are rateless erasure codes that can potentially generate unlimited coded data from the raw data [10]. The LT codes [19] are the first practical realization of fountain codes, and the core of the more recent Raptor codes [20]. The basic features of the LT codes are summarized as follows.

The encoding of an LT packet consists of two steps. Consider a total of k input packets, then

1) the encoder first randomly chooses integer $d \in [1,\ k]$ as the degree (number of input packets) of the coded packet according to a degree distribution probability; and
2) d input packets are independently and randomly selected from the batch of k packets. These d packets are XORed together to generate one LT coded packet.

To recover the original packets, the LT decoder adopts the belief propagation (BP) technique. With the encoding degree and packet index information of each coded packet, a bipartite graph is formed. The decoder starts by releasing packets with degree one. Then all edges connected to the degree-one packet(s) are removed. This is done recursively until no degree-one packet is left. If all k input packets are recovered, then the decoding is successful, otherwise, a failure is reported.

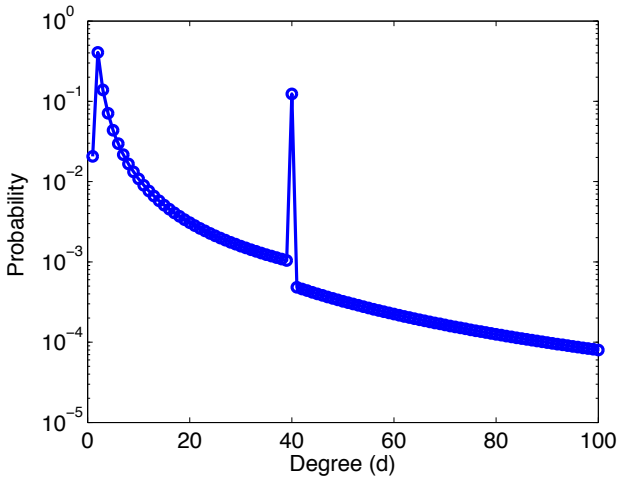

Fig. 1. An example of RSD with parameters: $k = 1000$, $c = 0.08$ and $\delta = 0.05$.

For an LT code to achieve high decoding success probability, the key is to design a good encoding degree distribution. In [19], Luby develops the RSD $\mu(x) = \sum_{i=1}^{k} \mu_i x^i$, where μ_i is the probability of choosing degree $d = i$.

Definition 1 (Robust Soliton Distribution) *With two parameters $\delta \in [0,1]$ and $c \geq 0$, the RSD can be computed as:*

$$\mu(x) = \frac{\rho(x) + \tau(x)}{\beta}, \tag{1}$$

where $\beta = \rho(1)+\tau(1)$ is a normalizing constant, $\rho(x) = x/k + \sum_{i=2}^{k} x^i/i(i-1)$, $\tau(x) = \sum_{i=1}^{k/R-1} Rx^i/ik + R\ln(R/\delta)x^{k/R}/k$, and $R = c\sqrt{k}\ln(k/\delta)$.

As proved in [19], with $k + \mathcal{O}(\sqrt{k}\ln^2(k/\delta))$ RSD encoded packets, the BP decoder can successfully recover all k input packets with probability of at least $1 - \delta$. One example of the RSD is shown in Fig. 1 with $c = 0.08$ and $\delta = 0.05$. Notice that the degree distribution is a fast decaying function of d with most distribution concentrating on the low degree orders, except for a spike at degree $d = k/R$.

B. DLT code construction

Different from the primitive LT codes, the DLT codes generate each packet with two layers of random encoding, as shown in Fig. 2. For a total of k input packets, the encoding process of the DLT code can be described as follows.

1) In the first layer, the k input packets are first randomly encoded in the same manner as the LT codes, but with a different degree distribution polynomial (DDP) $\theta(x)$, the output packets are termed as DLT-1 packets;
2) Then, the DLT-1 packets are considered as the input to the second layer random encoder with another DDP $\omega(x)$. The final output packets are called DLT-2 packets.

In addition, the DLT decoder utilizes a single layer BP algorithm as the LT decoder. To achieve good BP decoding performance, the key of the DLT code construction is to design two appropriate encoding DDPs $\theta(x)$ and $\omega(x)$ such that the

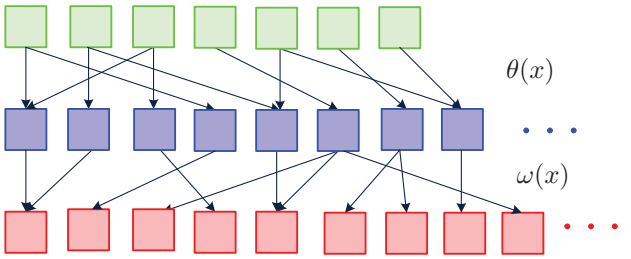

Fig. 2. The encoding diagram for a DLT code with two encoding DDPs of $\theta(x)$ and $\omega(x)$.

distribution of the DLT-2 packets resembles that of the LT codes $\mu(x)$. This can be mathematically expressed as:

$$\mu(x)=\omega(\theta(x)). \tag{2}$$

An intuitive approach is to decompose $\mu(x)$ into two valid polynomials. However, general polynomial decomposition is very challenging. In the literature, existing research has revealed that, for a uni-variable polynomial $f(x)$, analytical decomposition solutions do not always exist for arbitrary degree orders [21], while numerical decomposition algorithms cannot guarantee perfect match of high order coefficients [22]. In addition, to the best of our knowledge, none of existing methods can guarantee nonnegative decomposition solutions. Thus we will develop a nonnegative approximate decomposition method in the following.

By expanding the polynomial coefficients, (2) can be written in a matrix form as:

$$\boldsymbol{\Theta\omega}=\boldsymbol{\mu}, \tag{3}$$

where $\boldsymbol{\mu}=[\mu_1,\mu_2,\cdots,\mu_k]$, $\boldsymbol{\omega}=[\omega_1,\omega_2,\cdots,\omega_{D_\omega}]$ and $\boldsymbol{\Theta}$ is a $k\times D_\omega$ matrix,

$$\boldsymbol{\Theta}=\begin{bmatrix}\theta_1 & 0 & 0 & \cdots & 0\\ \theta_2 & \theta_1^2 & 0 & \cdots & 0\\ \theta_3 & 2\theta_1\theta_2 & \theta_1^3 & \cdots & 0\\ \vdots & \vdots & \vdots & \ddots & \vdots\\ \cdots & \cdots & \cdots & \cdots & \theta_1^{D_\omega}\\ \vdots & \vdots & \vdots & \ddots & \vdots\\ 0 & 0 & 0 & 0 & \theta_{D_\theta}^{D_\omega}\end{bmatrix}. \tag{4}$$

This equation set has nonlinear terms, which render the direct solution mathematically intractable. Notice that the nonlinearity only comes from $\boldsymbol{\Theta}$. If one can first determine an appropriate tentative solution of $\boldsymbol{\Theta}$, then $\boldsymbol{\omega}$ can be solved from a linear equation set. However, analysis in [23] indicates that the nonnegative exact solution to the over-determined equation set (3) does not exist for nontrivial D_θ and D_ω. Recall that the coefficients of RSD $\mu(x)$ are decaying in terms of the encoding degree ($i\geq 2$). Thus it is reasonable to match the dominant lower order terms, which leads to the following reduced decomposition problem.

Problem Statement 1 *For a given LT DDP $\mu(x)$ with maximum degree k, determine a nonnegative-coefficient polynomial $\theta(x)$ with $\theta(1)\leq 1$, such that the following linear equation set has a nonnegative solution $\boldsymbol{\omega}\in[0,\ 1)$ with $\omega(1)=1$,*

$$\tilde{\boldsymbol{\Theta}}\boldsymbol{\omega}=\tilde{\boldsymbol{\mu}}, \tag{5}$$

where $\tilde{\boldsymbol{\mu}}=[\mu_1,\ \mu_2,\ \cdots,\ \mu_{D_\omega}]$ and $\tilde{\boldsymbol{\Theta}}$ is a $D_\omega\times D_\omega$ lower-triangular truncated $\boldsymbol{\Theta}$ matrix of full-rank.

1) Valid choice of $\theta(x)$: Analysis in [24] reveals that the sufficient and necessary condition for nonnegative solution is: all equations, including the reduced ones, contain both positive and negative coefficients. By applying this to the coefficient matrix $\tilde{\boldsymbol{\Theta}}$ in the approximate decomposition (5), we can obtain the following.

Lemma 1 *To guarantee nonnegative solutions of $\boldsymbol{\omega}$ in* (5)*, the following condition must be satisfied:*

$$f(r,j)<0,\ j\geq 1,\ r>j, \tag{6}$$

where $f(r,j)=f(r,j-1)\theta_1^j-f(j,j-1)\tilde{\Theta}_{r,j}$ and $f(r,0)=-\mu_r$.

Proof: See Appendix I. ■

Due to the lower-triangular feature of the $\tilde{\boldsymbol{\Theta}}$ matrix, we can obtain the expression of $\boldsymbol{\omega}$ in terms of $f(r,j)$ as follows.

Lemma 2 *The solutions of $\boldsymbol{\omega}$ to* (5) *are represented as:*

$$\omega_j=-f(j,j-1)\theta_1^{-j(j+1)/2}. \tag{7}$$

Proof: See Appendix I. ■

Under the requirement of $\boldsymbol{\omega}\in[0,\ 1)$, we can obtain the rules for valid choices of $\theta(x)$ in the following proposition.

Proposition 1 *To guarantee that* (5) *has valid solutions, the coefficients of $\theta(x)$ must obey the following rules:*

- *For $j=1$, θ_1 needs to satisfy*

$$\theta_1^3-\mu_2\theta_1+\mu_1>0; \tag{8}$$

- *For $j\geq 2$, θ_j should be chosen in the range $[\theta_j^l,\theta_j^h]$, where*

$$\theta_2^l=\max\left\{\theta_1\frac{\mu_2-\theta_1^2}{\mu_1},\theta_1\frac{\mu_2-\sqrt{\mu_2^2-2\mu_1(\mu_3-\mu_1/\theta_1-\theta_1^3)}}{2\mu_1}\right\} \tag{9}$$

$$\theta_2^h=\min\left\{\frac{\mu_2\theta_1}{\mu_1},\ \theta_1\frac{\mu_2-\sqrt{\mu_2^2-2\mu_1\mu_3}}{2\mu_1}\right\}$$

$$\theta_j^l=\max\left\{\frac{g(j,j-1)-\theta_1^{j(j+1)/2}}{\mu_1\theta_1^{(j-2)(j+1)/2}},\frac{\theta_1^{(j-1)(j+2)/2}[\mu_1+\theta_1^{j+2}]-h(j,j-1)}{(2f(2,1)+j\mu_1\theta_2)\theta_1^{(j^2+j-4)/2}}\right\}$$

$$\theta_j^h=\min\left\{\frac{g(j,j-1)}{\mu_1\theta_1^{(j-2)(j+1)/2}},\frac{-h(j,j-1)}{(2f(2,1)+j\mu_1\theta_2)\theta_1^{(j^2+j-4)/2}}\right\}.$$

In these limits,

$$g(j,j-1)=\mu_j\theta_1^{j(j-1)/2}+\sum_{i=1}^{j-2}f(j-i,j-1-i)\tilde{\Theta}_{j,j-i}\theta_1^{(i-1)(2j-i)/2} \tag{10}$$

$$h(j,j-1)=\theta_1^{(j-1)(j+2)/2}[\mu_{j+1}\theta_1-j\mu_j\theta_2] + \sum_{i=1}^{j-2}\left[\tilde{\Theta}_{j+1,j-i}\theta_1-j\tilde{\Theta}_{j,j-i}\theta_2\right]f(j-i,j-i-1)\theta_1^{i(j-(i-1)/2)-1}. \tag{11}$$

Proof: See Appendix II. ■

2) Decomposition algorithm: For a smooth distribution $\mu(x)$, the approximate decomposition algorithm for Problem Statement 1 can be summarized as follows.

Algorithm 1: Degree distribution decomposition

Input: The target degree distribution $\mu(x)$
Result: The decomposed DDPs $\theta(x)$ and $\omega(x)$
Initialization: Set some initial value for $\alpha \in [0,\ 1]$;
while $\alpha < 1$ **do**
  for $j = 1$ *to* D_θ **do**
    if $j = 1$ **then**
    Choose a value for θ_1 that satisfies (8);
    else Compute the valid range $[\theta_j^l,\ \theta_j^h]$ for θ_j according to (9);
    Calculate $\theta_j = \alpha\theta_j^l + (1-\alpha)\theta_j^h$;
  end
  Compute $\boldsymbol{\omega}$ from (5) and determine the total probability $\omega(1)$;
  if $\omega(1) = 1$ **then** output the coefficients of $\theta(x)$ and $\omega(x)$, and break;
  else Increase $\alpha = \alpha + \delta_\alpha$;
end

III. Hybrid DLT Codes

In this section, we will investigate the DLT codes obtained from the classic RSD. Recall that the RSD has a spike at degree $d = k/R$. Notice from (11), an abrupt increase of μ_{j+1} may induce positive $h(j, j-1)$, which will result in $\theta_j^h < 0$, and an empty range for θ_j. Thus the spike in RSD will render an invalid range for θ_{d-1}. Therefore, direct application of Algorithm 1 without special treatment of the spike may fail to establish a valid RSD decomposition. The h-DLT codes are designed to address this issue by extracting a decomposable part of the distribution $\mu(x)$ for DLT encoding, while the remaining distribution is taken care of separately.

A. Encoding scheme

In the h-DLT codes, the data encoding is conducted in hybrid modes: two-layer cooperative DLT mode and one-layer direct LT mode. In the cooperative DLT mode, each packet will be encoded by both encoders; while in the direct LT mode, the packets are generated only by the first encoder. Besides, by adjusting the mode ratio, the h-DLT codes can control the encoding cost allocation between the first and second encoders.

With hybrid encoding, two degree distributions $\theta_1(x)$, $\theta_0(x)$ and an encoding ratio η are associated with the first encoder to generate both DLT-1 and LT packets. The second encoder will determine the encoding mode based on the type of individual packets.

1) At the first encoder, a binary random number generator is adopted to select an encoding mode, as shown in Fig. 3. With probability η, the encoder will choose the cooperative DLT mode and generate a DLT-1 packet with the encoding DDP $\theta_1(x)$; with probability $1-\eta$, the encoder will operate in the direct LT mode, and an LT packet is encoded with the DDP $\theta_0(x)$. All coded packets are the inputs to the second encoder.
2) At the second encoder, an encoding degree d is first randomly chosen with distribution $\omega(x)$. Then d packets are chosen from the inputs. If all selected packets are labeled as DLT-1, they are XORed together to generate an h-DLT packet; otherwise, one LT packet is output as an h-DLT packet, as shown in Fig. 4.

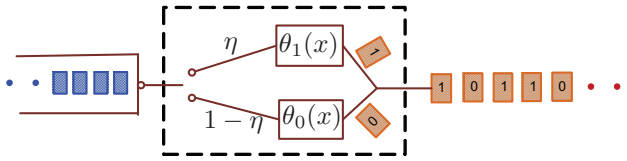

Fig. 3. The encoding diagram of the first encoder of the h-DLT codes.

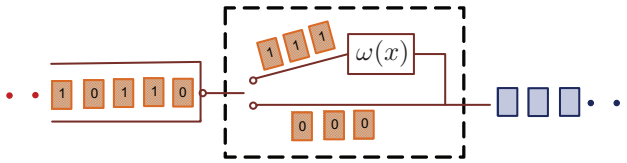

Fig. 4. The encoding diagram of the second encoder of the SD-DLT/h-DLT codes.

With this hybrid encoding scheme, the resultant degree distribution of the output packets and the average encoding degree of both encoders can be obtained as follows.

Proposition 2 *For an h-DLT code with a first-layer encoding DDP* $\theta(x) = \eta\theta_1(x) + (1-\eta)\theta_0(x)$ *and a second-layer DDP* $\omega(x)$, *the resultant degree distribution* $\hat{\mu}(x)$ *is computed as:*

$$\hat{\mu}(x) = \omega(\eta\theta_1(x)) + (1-\omega(\eta))\theta_0(x). \tag{12}$$

The average encoding degrees of the first encoder (C_1) *and second encoder* (C_2) *are:*

$$\begin{aligned} C_1 &= \theta'(1) = \eta\theta_1'(1) + (1-\eta)\theta_2'(1) \\ C_2 &= 1 - \omega(\eta) + \eta\omega'(\eta). \end{aligned} \tag{13}$$

Proof: With two layers of random encoding, the output degree distribution is:

$$\hat{\mu}(x) = \omega(\theta(x)) = \sum_{i=1}^{D_\omega} \omega_i \left(\eta\theta_1(x) + (1-\eta)\theta_0(x)\right)^i. \tag{14}$$

At the second encoder, any selection containing LT packets will directly result in an h-DLT packet. Thus,

$$\hat{\mu}(x) = \sum_{i=1}^{D_\omega} \omega_i \left[\eta^i(\theta_1(x))^i + \sum_{m=1}^{i} \binom{i}{m} \eta^{i-m}(1-\eta)^m\theta_0(x)\right], \tag{15}$$

which will lead to the expression in (12).

By evaluating $\theta'(1)$, we can readily obtain C_1. From (15), we can compute C_2 as:

$$C_2 = \sum_{i=1}^{D_\omega} i\omega_i\eta^i + (1 - \sum_{i=1}^{D_\omega} \omega_i\eta^i), \tag{16}$$

which can be simplified to (13). ■

Denote the resultant DDPs of the cooperative DLT mode and the direct LT mode as $\mu_1(x)$ and $\mu_2(x)$. From (12), we know that $\mu_1(x) = \omega(\eta\theta_1(x))$ and $\mu_2(x) = (1-\omega(\eta))\theta_0(x)$. The portion assigned to the cooperative DLT encoding is define as the mode ratio $\gamma = \mu_1(1)/\hat{\mu}(1) = \omega(\eta)$.

B. Hybrid distribution decomposition

Notice that the h-DLT codes require three distributions: $\theta_1(x)$, $\theta_0(x)$ and $\omega(x)$. To obtain these DDPs from a given RSD, we first construct a smooth distribution $\tilde{\mu}(x)$ by removing the distribution spike. Then a fraction of $\tilde{\mu}(x)$ is allocated to the DLT mode $\mu_1(x)$ for decomposition, and the remaining is assigned to $\mu_2(x)$ as direct LT mode. By adjusting this fraction, one can obtain a hybrid RSD decomposition that satisfies the target encoding cost ratio $\alpha_C = C_1/C_2$. The decomposition technique is described as follows.

Algorithm 2: Hybrid RSD Decomposition

Input: The target RSD $\mu(x)$ and encoding cost ratio α_C^t
Result: The decomposed DDPs $\theta(x)$ and $\omega(x)$
Initialization:
Construct a smooth distribution $\tilde{\mu}(x) = (\rho(x) + \tilde{\tau}(x))/\beta$ with $\tilde{\tau}(x) = \sum_{i=1}^{k/R}(R/ik)x^i$;
Choose a tentative ratio $\tilde{\gamma}$;
repeat
  Compute $\mu_1(x) = \tilde{\gamma}\tilde{\mu}(x)$;
  Decompose $\mu_1(x)$ into $\tilde{\theta}_1(x)$ and $\omega(x)$ using Algorithm 1;
  Compute $\eta = \tilde{\theta}_1(1)$, and $\theta_1(x) = \tilde{\theta}_1(x)/\eta$;
  Calculate $\theta_0(x) = (\mu(x) - \omega(\tilde{\theta}_1(x)))/(1-\omega(\eta))$;
  Determine the encoding cost ratio $\alpha_C = C_1/C_2$;
  Increase $\tilde{\gamma} = \tilde{\gamma} + \delta_\gamma$.
until $\alpha_C = \alpha_C^t$;
Compute $\theta(x) = \eta\theta_1(x) + (1-\eta)\theta_0(x)$.

Notice from Algorithm 2 that the direct LT mode $\theta_0(x)$ captures all non-decomposed distribution. Thus, the resultant distribution of the h-DLT codes is identical to the target RSD, i.e. $\hat{\mu}(x) = \mu(x)$.

In summary, the h-DLT codes obtained from the RSD is featured with two layers of encoding, but a single layer of decoding, together with flexible computation cost allocation. Thus they are well suited for cooperative relay communications for much better energy efficiency than the concatenated fountain codes based schemes. In addition, by adapting computation allocation to the residual energy of the heterogeneous cooperative nodes, the h-DLT codes can prolong the cooperative network lifetime.

IV. Hybrid DLT Codes based Cooperative Relay Communications

Cooperative relay communications enable long-distance reliable data delivery. However, the cooperative transmission schemes based on traditional FEC codes suffer from large latency and high energy cost. To address these issues, we will design an h-DLT based cooperative relay communication (DLT-CC) protocol in this section.

A. System setup

In the DLT-CC scheme, the source and the relay(s) will adopt the first and second-layer encoding of the h-DLT codes, respectively. In order to choose an h-DLT code with appropriate computation allocation ratio for the cooperative network, the source will first broadcast the request for relaying. The available intermediate nodes will reply with their residual energy, distance to the destination and etc. Based on the feedback, the source will first choose a set of relay nodes according to certain performance criteria (see, e.g., [5], [6]). Then, according to the residual energy ratio α_E between the source and the chosen relays, an optimal h-DLT code is obtained with Algorithm 2 such that $\alpha_C^t = \alpha_E$.

B. Transmission protocol

The DLT-CC protocol consists of three parts. Without loss of generality, time domain multiple access is assumed.

1) Source encoding and broadcast: With k data packets to be transmitted, the source first generates coded packets using the first-layer DDP of the h-DLT code $\theta(x)$. A one-bit ID is attached to each coded packet to indicate its encoding mode: LT ($ID = 0$) or DLT ($ID = 1$). The packets are continuously generated and broadcast to the relays/destination in the source transmission time slots. The transmission stops until ACKs are received from all relays.

2) Relay encoding and cooperative forwarding: At the relay, each received packet at the physical layer first undergoes an error detection (e.g. cyclic redundancy check (CRC)) process. If the CRC check succeeds, the packet will be stored and an h-DLT packet is generated using encoding degree distribution $\omega(x)$ when D_ω packets are accumulated. However, if a received packet fails the CRC check, the packet is dropped, and a new h-DLT packet is generated from the stored data. In the next time slot, each relay will forward the h-DLT packet to the destination. Each relay keeps forwarding h-DLT packets until an ACK is received from the destination. The ACK is also relayed to the source.

3) Destination decoding: At the destination, after CRC check, each correctly received packet is forwarded to the BP decoder to recover the source data, and all erroneous packets are deleted. After all k source packets are decoded, an ACK is sent back to the relays.

C. Performance of DLT-CC

To verify the benefits of the DLT-CC scheme, we analyze and simulate the performance of the system. The results are compared with existing schemes in the literature.

1) End-to-end latency: The end-to-end latency of a cooperative communication system consists of two parts: the total data packet transmission time and round-trip control time. Consider a total of k source packets, we can compute the latency T^L as:

$$T^L(p_1, p_2, k) = t_p N^C(p_1, p_2, k) + t_{RTT} N^R(p_1, p_2, k), \qquad (17)$$

where t_p and t_{RTT} are the transmission time of each packet and end-to-end round-trip time (RTT), N^C and N^R are the total numbers of packet transmission and retransmission requests, p_1 and p_2 are the average packet erasure rates on the source-relay and relay-destination links.

In the DLT-CC scheme, the transmitters can adapt to the channel erasure rate by continuously transmitting coded packets until a feedback message is received. Thus only one round trip is needed, $N_{\text{DLT}}^R = 1$. On the other hand, the average number of total transmissions is:

$$N_{\text{DLT}}^C(p_1, p_2, k) = \frac{2k(1+\epsilon)}{1-p_2}. \qquad (18)$$

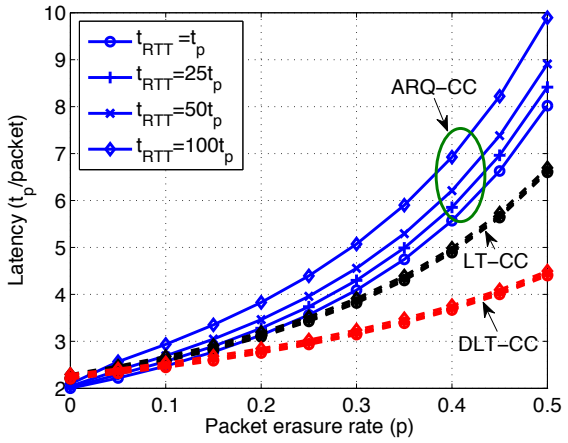

Fig. 5. The average transmission latency per packet for the ARQ, LT and DLT based cooperative transmission schemes.

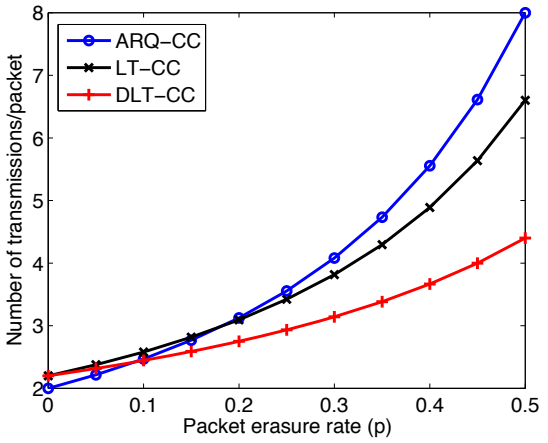

Fig. 6. The average number of transmissions per packet for the ARQ, LT and DLT based cooperative transmission schemes.

To illustrate the benefits of adopting an h-DLT code, we compare the results with two other traditional schemes: ARQ-based cooperative communication (ARQ-CC) and LT-based hybrid ARQ scheme (LT-CC). In the ARQ-CC scheme, no data encoding is adopted, and the destination will send back NACK messages to the source to request the lost packets for transmission reliability; In the LT-CC scheme, the source data is encoded with an LT code. The source will keep sending coded data to the destination with the relay forwarding until the destination sends back an ACK.

In classic ARQ based transmissions, the error-prone wireless channel incurs frequent retransmissions. For a transmission window of size k, the total number of retransmissions can be computed recursively as:

$$N^R_{\text{ARQ}}(p_1,p_2,k)=\frac{1}{1-p^k}\left[1+\sum_{i=1}^{k-1}\binom{k}{i}p^i(1-p)^{k-i}N^R_{\text{ARQ}}(p,i)\right].$$

And the end-to-end total number of transmissions is:

$$N^C_{\text{ARQ}}(p_1,p_2,k)=\frac{2}{1-p^k}\left[k+\sum_{i=1}^{k-1}\binom{k}{i}p^i(1-p)^{k-i}N^C_{\text{ARQ}}(p,i)\right], \quad (19)$$

where $p=p_1+p_2-p_1p_2$.

For the LT-CC scheme, the source will generate all redundant packets to counter erasures on both links, thus the total number of packet transmissions is:

$$N^C_{\text{LT}}(p_1,p_2,k)=\frac{k(1+\epsilon)}{(1-p_1)(1-p_2)}+\frac{k(1+\epsilon)}{1-p_2}=\frac{k(1+\epsilon)(2-p_1)}{(1-p_1)(1-p_2)}, \quad (20)$$

and the number of retransmissions is $N^R_{\text{LT}}=1$.

Assume $p_1=p_2=p$ for representation simplicity, we compute the average latency per packet for all three systems and for different t_{RTT}/t_p ratios according to (17). The results are plotted in Fig. 5, where the latency value is shown in terms of t_p. Notice that the DLT-CC scheme entails the smallest latency, and it is not sensitive to the t_{RTT}/t_p ratio. In the ARQ-CC system, the latency increases significantly with the t_{RTT}/t_p ratio. This indicates that our DLT-CC scheme is more beneficial for communication systems with large t_{RTT}/t_p ratio, such as underwater acoustic communications. In addition, the DLT-CC system also outperforms the LT-CC scheme with reduced latency. Because when an erasure occurs on the source-relay link, the relays in DLT-CC will generate redundant packets, while they keep silent in LT-CC.

2) Communication cost: The total energy consumption of a cooperative relay system consists of two parts: the data communication energy and the node computation cost. Here, we will first evaluate the communication energy in terms of the total number of packet transmissions.

With the analytical results in (18), (19) and (20), we can compute the average number of transmissions per packet for all three schemes with respect to different packet erasure rates. As shown in Fig. 6, the DLT-CC scheme requires the smallest communication cost. As the erasure rate increases, more communication energy can be saved by the DLT-CC scheme compared to other schemes.

For cooperative schemes using different decomposed LT codes, their communication energy difference is determined by the decoding overhead ϵ according to (18).

3) Decoding overhead: For a target RSD $\mu(x)$ with parameters $k=1000$, $c=0.08$ and $\delta=0.05$, we obtain the corresponding h-DLT distributions using Algorithm 2 for different mode ratios $\gamma=0.8,\ 0.6,\ 0.4$, and the distributed LT code in [18]. To illustrate the performance difference, we simulate the complementary cumulative distribution functions (CDF) of the required overhead (Δ) for successful decoding in Fig. 7. Due to space limit, only the result for $\gamma=0.4$ is included. As expected, the h-DLT code performs better than the distributed LT code, because the resultant degree of the h-DLT code is identical to the RSD, while there is some difference for the distributed LT code [18]. This indicates that the DLT-CC scheme outperforms the one using the distributed LT code with less communication energy consumption. In addition, compared to the primitive LT code, some performance degradation is also observed for the h-DLT codes. The degradation comes from the degree reduction induced by packet collision when the selected DLT-1 packets contain the same raw packets at the second layer. However, the small gap confirms that such events are very rare.

4) Computation complexity: The DLT-CC scheme is designed with flexible computation allocation. We compute the average encoding degree at each node for the DLT-CC

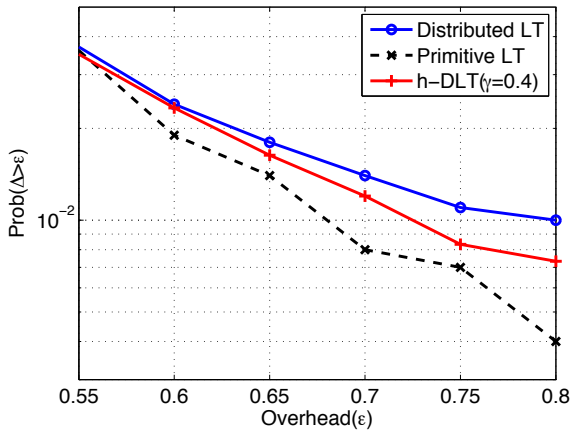

Fig. 7. The complementary cumulative distribution function of required overhead (Δ) for successful decoding for the distributed LT, primitive LT and h-DLT codes. The system parameters are: $k = 1000$, $c = 0.08$ and $\delta = 0.05$.

TABLE I
THE AVERAGE ENCODING DEGREE

Code Type	1st layer average encoding degree (C_1)	2nd layer average encoding degree (C_2)
h-DLT(γ=0.8)	2.85	3.47
h-DLT(γ=0.6)	2.94	3.06
h-DLT(γ=0.4)	3.58	2
Distributed LT	5.90	1.86
Concatenated LT	11.64	11.64

schemes using the h-DLT codes with different mode ratios γ. Based on (13), the computation costs are computed and listed in Table I. Observe that, as γ decreases, more encoding cost shifts from the relay to the source as expected.

To further reveal the benefits of our DLT-CRC scheme in computation cost, we compare it with other fountain code based communication protocols in the literature. The results are listed in Table II. Clearly, the DLT-CC scheme requires the least computation cost for all nodes. For example, when $\gamma = 0.4$, the source and the relay(s) can save about 69% and 82% of the computation compared to the concatenated encoding scheme. Besides, the destination requires only half of the decoding cost. Therefore, the DLT-CC protocol is expected to prolong the cooperative network lifetime with reduced computation and adaptive energy allocation.

V. Conclusions

In this work, we investigated decomposed LT codes for cooperative relay communications. The two-layer DLT encoding scheme is suitable for the dual-hop cooperative communications to facilitate reliability control with reduced latency and energy consumption. Extensive analyses were carried out to develop valid encoding distribution decomposition methods. Furthermore, the h-DLT codes, which enable flexible computation cost allocation between two encoders, were developed for the RSD. Finally, we designed an h-DLT-assisted cooperative relay communication scheme, which seamlessly incorporates the h-DLT codes into the dual-hop data transmission. This scheme also takes into account the heterogeneous node residual energy to prolong the network lifetime. Analyses and comparisons confirm that our proposed scheme significantly reduces the transmission latency and energy consumption.

TABLE II
THE AVERAGE COMPUTATION COST

Scheme	Source	Relay	Destination
Random linear code [15], [16]	$\mathcal{O}(k^2)$	$\mathcal{O}(k^2)$	$\mathcal{O}(k^3)$
Decode-Reencode [3], [11]	$\mu'(1)k$	$\mathcal{O}(k\ln k)+\mu'(1)k$	$\mathcal{O}(k\ln k)$
Concatenated LT [13], [14]	$\mu'(1)k$	$\mu'(1)k$	$2\mathcal{O}(k\ln k)$
DLT-CC	C_1k	C_2k	$\mathcal{O}(k\ln k)$

Appendix I: Proof of Lemma 1

Following the theorem in [24], we can prove the requirements on $\theta(x)$ as follows.

In the first step, move $\tilde{\boldsymbol{\mu}}$ in (5) to the left side of the equation set. Notice that, in the r^{th} equation, the only negative term is $-\mu_r$ and all others are positive. Thus the mixed negative and positive condition is satisfied for each equation. Define $f(r,0) = -\mu_r$.

Then we can proceed to the second step to reduce the D_ω equations to $D_\omega - 1$. In row $r=1$, $\sum_{k=1}^{n} \tilde{\Theta}_{1,k}\omega_k = \mu_1$, thus we rearrange other rows ($r>1$) as: $\sum_{k=1}^{n} \tilde{\Theta}_{r,k}\omega_k = \mu_r$, and apply the multiplication rule on both sides,

$$\sum_{k=1}^{n} \left(\mu_1\tilde{\Theta}_{r,k} - \mu_r\tilde{\Theta}_{1,k}\right)\omega_k = 0, \qquad r>1. \tag{21}$$

Since $\tilde{\Theta}_{1,1} = \theta_1$ and $\tilde{\Theta}_{1,k} = 0,\ k>1$, only the first term in (21) for each r can possibly be negative. In order to assure the positive solution, the following condition must be guaranteed: $f(r,1) = \mu_1\tilde{\Theta}_{r,1} - \mu_r\tilde{\Theta}_{1,1} < 0$.

Under this, we can proceed to reduce the D_ω–1 equations by 1. Rearrange (21) as: $\sum_{k=2}^{n}\left(\mu_1\tilde{\Theta}_{r,k}\right)\omega_k = -f(r,1)\omega_1,\ r>1$, and multiply the $r=2$ equation to all others:

$$\sum_{k=2}^{n}\left(-f(2,1)\tilde{\Theta}_{r,k} - (-f(r,1))\tilde{\Theta}_{2,k}\right)\omega_k = 0, r>2. \tag{22}$$

In the second row of $\tilde{\boldsymbol{\Theta}}$, $\tilde{\Theta}_{2,2} = \theta_1^2$ and $\tilde{\Theta}_{2,k} = 0,\ k>2$, thus the $k=2$ term must be negative: $f(r,2) = -f(2,1)\tilde{\Theta}_{r,2} - (-f(r,1))\tilde{\Theta}_{2,2} < 0$. Continue this process, we can obtain that, in the j^{th} elimination step,

$$\sum_{k=j}^{n}\left(-f(j,j-1)\tilde{\Theta}_{r,k} - (-f(r,j-1))\tilde{\Theta}_{j,k}\right)\omega_k = 0,\ r>j. \tag{23}$$

The fact of $\tilde{\Theta}_{r,k} = 0,\ k>r$ renders that

$$f(r,j) = f(r,j-1)\tilde{\Theta}_{j,j} - f(j,j-1)\tilde{\Theta}_{r,j} < 0, r>j. \tag{24}$$

Thus Lemma 1 is proved.

In addition, the first equation in (23) ($r = j+1$) can be expressed as: $-f(j,j-1)\tilde{\Theta}_{j+1,j+1}\omega_{j+1} = -f(j+1,j)\omega_j$, which implies that $\omega_{j+1}/\omega_j = f(j+1,j)/f(j,j-1)\theta_1^{-(j+1)}$. Consequently, we can obtain the results in Lemma 2.

Appendix II: Proof of Proposition 1

As a valid solution to (5), the value of $\boldsymbol{\omega}$ must satisfy $0 \le \boldsymbol{\omega} < 1$. From (24), we have:

$$f(j,j-1) = \left[\mu_1\theta_1^{(j-2)(j+1)/2}\right]\theta_j - \mu_j\theta_1^{j(j-1)/2} - \sum_{i=1}^{j-2} f(j-i,j-i-1)\tilde{\Theta}_{j,j-i}\theta_1^{(i-1)(2j-i)/2}. \tag{25}$$

With the expression of ω_j in Lemma 2 and the equality above, the constraint on ω_j is transferred to θ_j as:

$$\frac{g(j,j-1)-\theta_1^{j(j+1)/2}}{\mu_1\theta_1^{(j-2)(j+1)/2}}<\theta_j<\frac{g(j,j-1)}{\mu_1\theta_1^{(j-2)(j+1)/2}}, \tag{26}$$

where $g(j,j-1)$ is defined in (10). By choosing a valid value of each θ_j within this range starting from $j=1$ to $j=D_\theta$, a feasible solution of $\boldsymbol{\omega}$ can be obtained.

In order to have a valid range in (26), the left hand side needs to be less than 1 and the right hand side should be larger than 0. These correspond to $0<g(j,j-1)<\theta_1^{(j-2)(j+1)/2}[\mu_1+\theta_1^{j+1}]$. Notice that the $\tilde{\boldsymbol{\Theta}}$ elements in $h(j-1,j-1)$ are obtained with $\theta_k=0,\ k\geq j-1$. Thus the constraint on $g(j,j-1)$ poses extra limits on θ_{j-1}. By changing the index from j to $j+1$, we have,

$$0<\left[(2f(2,1)+j\mu_1\theta_2)\theta_1^{(j^2+j-4)/2}\right]\theta_j+h(j,j-1)<\theta_1^{(j-1)(j+2)/2}[\mu_1+\theta_1^{j+2}].$$

For a choice of $\theta_2 < 2\mu_2\theta_1/(j+2)\mu_1$, the constraints on $\theta_j,\ j>2$ can be obtained.

For $j=2,\ 0<\omega_2<1$ renders $\theta_1(\mu_2-\theta_1^2)/\mu_1<\theta_2<\mu_2\theta_1/\mu_1$. The limit for θ_2 is computed from $0<g(3,2)<\theta_1^2[\mu_1+\theta_1^4]$.

For $j=1$, the constraint on $g(2,1)$ requires $0<g(2,1)=\mu_2\theta_1<(\mu_1+\theta_1^3)$. The left side is automatically satisfied, but the right side leads to $\theta_1^3-\mu_2\theta_1+\mu_1>0$. Putting all constraints for θ_j together leads to Proposition 1.

REFERENCES

[1] J. N. Laneman, D. N. C. Tse, and G. W. Wornell, "Cooperative diversity in wireless networks: Efficient protocols and outage behavior," *IEEE Trans. Inf. Theory*, vol. 50, no. 12, pp. 3062–3080, Dec. 2004.

[2] T. Wang, A. Cano, G. B. Giannakis, and J. N. Laneman, "High-performance cooperative demodulation with decode-and-forward relays," *IEEE Trans. Commun.*, vol. 55, no. 7, pp. 1427–1438, Jul. 2007.

[3] J. Castura and Y. Mao, "Rateless coding for wireless relay channels," *IEEE Trans. Wireless Commun.*, vol. 6, pp. 1638–1642, May 2007.

[4] M.-H. Lu, P. Steenkiste, and T. Chen, "Time-aware opportunistic relay for video streaming over WLANs," in *IEEE International Conf. on Multimedia and Expo*, Beijing, China, Jul. 2–5 2007.

[5] Y. Wei, F. R. Yu, and M. Song, "Distributed optimal relay selection in wireless cooperative networks with finite-state markov channels," *IEEE Trans. Veh. Technol.*, vol. 59, pp. 2149–2158, Jun. 2010.

[6] W. Zhang, D. Duan, and L. Yang, "Relay selection from a battery energy efficiency perspective," *IEEE Trans. Wireless Commun.*, 2011 (to appear).

[7] P. Liu, Z. Tao, Z. Lin, E. Erkip, and S. Panwar, "Cooperative wireless Comm.: a cross-layer approach," *IEEE Trans. Wireless Commun.*, vol. 13, pp. 84–92, Aug. 2006.

[8] B. Zhao and M. C. Valenti, "Practical relay networks: a generalization of hybrid-ARQ," *IEEE J. Sel. Areas Commun.*, vol. 23, pp. 7–18, Jan. 2005.

[9] M. Luby, M. Mitzenmacher, A. Shokrollahi, and D. Spielman, "Efficient erasure correcting codes," *IEEE Trans. Inf. Theory*, vol. 47, pp. 569–584, Feb. 2001.

[10] D. J. C. MacKay, *Information Theory, Inference, and Learning Algorithms*. Cambridge University Press, 2003.

[11] X. Liu and T. J. Lim, "Fountain codes over fading relay channels," *IEEE Trans. Wireless Commun.*, vol. 8, pp. 3278–3287, Jun. 2009.

[12] A. F. Molisch, N. B. Mehta, J. S. Yedidia, and J. Zhang, "Performance of fountain codes in collaborative relay networks," *IEEE Trans. Wireless Commun.*, vol. 6, no. 11, pp. 4108–4119, Nov. 2007.

[13] R. Gummadi and R. S. Sreenivas, "Relaying a fountain code across multiple nodes," in *Info. Theory Workshop (ITW '08)*, Porto, Portugal, May 5–9 2008, pp. 149–153.

[14] P. Pakzad, C. Fragouli, and A. Shokrollahi, "Coding schemes for line networks," in *IEEE International Symposium on Info. Theory*, Adelaide, Australia, Sep. 4–9 2005.

[15] A. Tarable, I. Chatzigeorgiou, and I. J. Wassell, "Randomly select and forward: Erasure probability analysis of a probabilistic relay channel model," in *IEEE Info. Theory Workshop*, Taormina, Italy, Oct. 11–16 2009, pp. 41–45.

[16] H. Wicaksana, S. Ting, and Y. Guan, "Spectral efficient half duplex relaying for fountain code with wireless network coding," in *IEEE International Conf. on Comm. Workshops*, Beijing, China, May 19–23 2008, pp. 295–299.

[17] D. Sejdinović, R. J. Piechocki, and A. Doufexi, "AND-OR tree analysis of distributed LT codes," in *IEEE Info. Theory Workshop on Networking and Info. Theory (ITW)*, Volos, Greece, Jun. 10–12 2009.

[18] S. Puducheri, J. Kliewer, and T. E. Fuja, "The design and performance of distributed LT codes," *IEEE Trans. Inf. Theory*, vol. 53, no. 10, pp. 3740–3754, 2007.

[19] M. Luby, "LT codes," in *43rd Symposium on Foundations of Computer Science (FOCS)*, Vancouver, BC, Canada, Nov. 16–19 2002.

[20] A. Shokrollahi, "Raptor codes," *IEEE Trans. Inf. Theory*, vol. 52, no. 6, pp. 2551–2567, Jun. 2006.

[21] V. S. Alagar and M. Thanh, "Fast polynomial decomposition algorithms," *EUROCAL'85 Lecture Notes in Computer Science*, vol. 204, pp. 150–153, 1985.

[22] R. M. Corless, M. W. Giesbrecht, D. J. Jeffrey, and S. M. Watt, "Approximate polynomial decomposition," in *International Symposium on Symbolic and Algebraic Computation*, Vancouver, BC, Canada, Jul. 28–31 1999, pp. 213–220.

[23] R. Cao and L. Yang, "On the design of decomposed Raptor codes and the application in data-centric storage," *IEEE Trans. Comm.*, 2011 (submitted).

[24] L. L. Dines, "On positive solutions of a system of linear equations," *The Annals of Mathematics, 2nd Series*, vol. 28, no. 1/4, pp. 386–392, 1927.

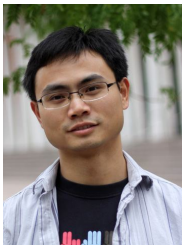

Rui Cao (S'07) received his B.S. degree in Physics from Nanjing University, Nanjing, China, in 2003, and M.S. degree in Physics from Arizona State University, Tempe, Arizona, in 2006. He is currently pursuing the Ph.D degree with the Department of Electrical and Computer Engineering, University of Florida, Gainesville, Florida. His current research interests include wireless communications and distributed data storage.

Liuqing Yang (S'02-M'04-SM'06) received her Ph.D. degree from the University of Minnesota, Minneapolis in 2004. After that, she joined the University of Florida, Gainesville, and became an Associate Professor in 2009. Since 2010, she has been with Colorado State University. Her current research interests include signal processing, communications theory and networking.